Linking technical geothermal potential from borehole heat exchangers and heating demand scenarios on a regional scale

Johannes M. Miocic[1,2], Marc Krecher[3]

[1]Energy and Sustainability Research Institute, University of Groningen, Energy Academy, Nijenborgh 6, 9747 AG Groningen, The Netherlands

[2]Institute of Earth and Environmental Sciences, University of Freiburg, Albertstr. 23b, 79104 Freiburg, Germany

[3]bnNetze GmbH (Badenova Group), Tullastr. 61, 79108 Freiburg, Germany

Correspondence to: j.m.miocic@rug.nl

Abstract

Extracting shallow geothermal energy using borehole heat exchangers (BHEs) can help decarbonising the residential heating sector. To assist urban planers and policy makers in developing carbon-neutral heating plans the regional technical shallow geothermal potential must be analysed. Here, we propose a methodology to estimate the technical geothermal potential of BHE fields on a regional scale while taking potential thermal interference between BHEs, geological conditions, as well as space available for BHE installation into account. The number of BHEs placed is maximized and heat extraction rate from each BHE is optimized taking regional regulations into account. When the methodology is applied to the German state of Baden-Württemberg on a building-block scale, results suggest an annual technical potential of 33.5 TWh. This technical geothermal potential is then linked to heating demand scenarios per building block and the results show that, depending on the renovation status of the buildings, between 44 % and 93 % of all building blocks can heated using only BHEs. This allows for the identification of building blocks in which BHEs are not able to meet the heating demand and where other means of heat supply will be needed.

Keywords: Shallow geothermal energy; Borehole heat exchangers; Technical potential estimation; Heating demand

1 Introduction

In order to achieve greenhouse gas emission reduction targets set out in the Paris agreement (UNFCCC, 2015) and the EU's climate neutrality goal by 2050 as outlined in the European Green Deal (European Parliament, 2020), a large-scale transformation to renewable energies in the heating and cooling sector is needed. Energy used for heating and cooling accounts for the majority of the final energy use per household (79 % in EU households), and about 30 % of all energy consumed in the

European Union is used for space heating and hot water generation (Fleiter et al., 2017). The bulk energy used in the heating and cooling sector is still generated from fossil fuels (75% of heating and cooling in the EU in 2018), and in order to meet the climate and energy goals, on both EU and country level, the sector is in high need for decarbonisation and reduction of energy consumption. Widely discussed options for heating and cooling in future renewable energy systems include district heating (Lund et al., 2010), decentralization of energy systems (Orehounig et al., 2015), and the widespread use of heat pumps (Lund, 2007). For the latter, shallow geothermal energy systems are particularly appealing as they are more efficient than water-air heat pumps as the ground has a more stable temperature than the ambient air. Therefore, a widespread global roll-out of shallow geothermal energy utilization would allow for a strong carbon emission reduction of the heating sector (Lund and Boyd, 2016).

Shallow geothermal energy systems provide heating and/or cooling by exchanging heat with the shallow subsurface either via an open system, where ground water is accessed and acts as a heat carrier, or a closed system, where a synthetic heat carrier fluid is circulated through a closed tubing system in the ground for heat exchange. Both open and closed systems employ heat pumps to extract heat from the carrier fluid and supplying heating applications. While horizontal closed-loop systems can be installed, more commonly ground source heat pumps (GSHP) are set up with vertical boreholes heat exchangers (BHE). GSHPs are particularly interesting for areas with a low heat demand density for which a connection to a district heating network is not economically or environmentally efficient (Tissen et al., 2021).

In recent years, the sustainability and long-term effects of shallow geothermal energy usage has been addressed in many studies. High BHE densities can lead to interference between single boreholes (Meng et al., 2019; Vienken et al., 2015; Zhang et al., 2018) and decreasing ground temperatures may lead to a decrease in GSHP efficiency over time (Li et al., 2014; Patton et al., 2020). When shallow geothermal systems are also used for space cooling heat is introduced into the subsurface which leads to increased groundwater temperatures which in turn may lead to subsurface urban heat islands under densely populated areas (Menberg et al., 2013; Rivera et al., 2017). Numerous studies have explored the feasibility of geothermal use in urban areas with various approaches (Casasso and Sethi, 2016; Luo et al., 2018; Noorollahi et al., 2017), often using geographic information systems in combination with analytical or numerical models. These studies can support urban planners and policy makers, however to identify areas particularly suitable for GSHPs and to determine spatially defined regional differences regional studies of the technical geothermal potential are needed.

To date most studies that assess the regional-scale potential of geothermal energy estimate the theoretical potential, which is defined as the physically available energy in a given ground volume (Bayer et al., 2019), instead of the technical potential, which is the technically extractable heat with consideration of the built environment and the interference between boreholes. Such studies include the estimation of thermal conductivity on a large-scale as the entire European continent (Bertermann et al., 2015) or ground temperatures across the whole of Canada (Majorowicz et al., 2009). Other studies quantify regional technical potential of single boreholes with different approaches (Casasso and Sethi, 2016; Galgaro et al., 2015; Tissen et al., 2019a) but lack to take the interaction and interference between boreholes into account. Only one recent study estimates the technical potential on a regional scale (Walch et al., 2021), however it fails to link the geothermal potential to the heating demand.

A different approach was developed in 2014 for the purposes of municipal energy consulting by the regional energy supplier badenova AG & Co. KG (Krecher 2014). Based on a self-developed GIS-based analysis tool, it was possible to calculate the maximum possible energy output of borehole heat exchangers to satisfy the energy demand on the residential building level. Borehole and geothermal probe parameters are adopted to the surrounding conditions, taking also the interference between boreholes into account. This makes it possible to promote the use of geothermal heating at the level of residential quarters, considering local risks regarding the geological and subsoil conditions to reduce the inhibition threshold of the applicants. Based this previous work, we estimate the technical geothermal potential of vertical heat exchangers of GSHPs on a more regional level and compare it to three different demand scenarios for residential buildings. We calculate the maximum number of BHEs that can be placed on a building block scale while taking the build environment into account. For the technical geothermal potential, the thermal interference between BHEs is included by estimating g-functions on a building-block level which allows for a rapid calculation of the technical geothermal potential. Heat extraction rates are maximised while considering federal and state restrictions on BHE depth as well as ground and fluid temperatures. Within this study, vertical closed-loop GSHP systems which is the most widely used type of system in Germany are considered. Groundwater flow, possible re-charging of the subsurface with heat from solar thermal generators and space cooling during summer days are neglected in the presented model and thus the estimated geothermal potential can be regarded as conservative. This potential is then linked to three different demand scenarios which take building renovation status into account. This allows for identification of building blocks in which GSHP systems can supply all the demanded heat as well as for determination of building blocks for which even for a low heat demand scenario additional means of heating supply are needed.

2 Material and Methods

2.1 Study area

The state of Baden-Württemberg is located in the south-west of Germany and is its third largest state both by population (11.07 million) and area (35.751 km²) (Fig. 1). It has a diverse landscape, with dominant features being (1) the Upper Rhine Valley in the west, (2) the mountain range of the Black Forest which rises to the east of the valley, (3) the south German Scarplands north and east of the mountain range, (4) the high plateau of the Swabian Alb in the east of the Scarplands, (5) and the foothills of the Alps in the south-east of the state. This landscape is the result of a hundreds of million years long geological evolution and outcropping rocks cover most of the geological periods, ranging from Pre-Cambrian to Quaternary rocks (Geyer et al., 2011). The highest elevations can be found in the Black Forest (1493 m) while in the northern Upper Rhine Valley has elevations as low as 85 m above sea level. The location within Europe results in a more maritime climate in the west of the state and a continental climate in the east of the state. The Upper Rhine Valley has some of the warmest annual mean temperatures of all of Germany (>10° C) while in the Black Forest mean annual temperatures can be lower than 4°C.

The state has adopted legislation to reduce its greenhouse gas emissions by 42 % by 2030 and by 90 % by 2050 compared to emission in 1990. One key aspect of the legislation is that all municipalities have to (1) report their energy usage annually and municipalities with a population >20.000 (2) have to develop a municipal heating plan (KSG BW, 2013). These heating plans will form the base for climate-neutral heating supply in 2050. In 2017 around 90 % of the final energy consumption of households in Baden-Württemberg was from fossil fuels, with heating predominantly supplied by heating oil and natural gas (Schweizer, 2019). In 2019 around 43.000 GSHP systems were operating in the state, with annually around 3000 more systems being installed. The implementation of new GSHP systems must follow particularly strict regulations in this region due to several prominent damage events where improper installation of BHEs in areas with complex geology led to surface uplift/subsidence (Baden-Württemberg, 2018).

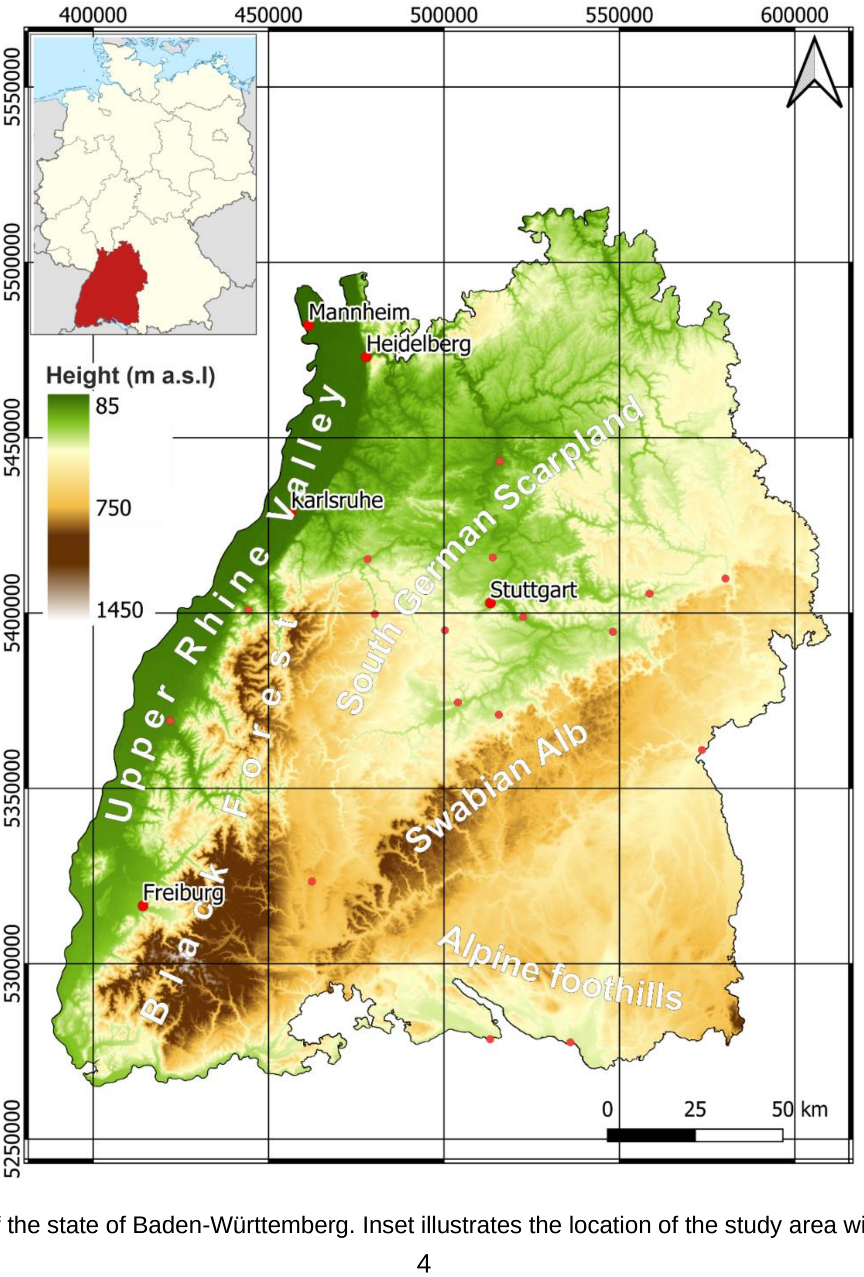

Figure 1: Map of the state of Baden-Württemberg. Inset illustrates the location of the study area within Germany.

2.2 Input data

Heating demand of residential buildings in Baden-Württemberg was provided as shape file on a building-bloc scale by the ministry of environment, climate and energy. The same data can be accessed, but not downloaded, online (www.energieatlas-bw.de). This heating demand data is based on a census on building type, year of construction and living area in the year 2011 as well as studies on heating demand of building types and ages. The Energieatlas provides three different heating demand scenarios: "as is" which reflects the heating demand at the year of construction but with coated double glazing independently of the construction year, "conventional renovation" which assumes a 12 cm insulation of roof and walls as well as coated double glazing, and "forward-looking renovation" which roughly translates to a KfW-55 efficiency house with a wall insulation of 18 cm, roof insulation of 24 cm, triple glazing, and a heat pump for heating and hot water.

Data on building layouts, roads, railways, and surface waters are freely accessible as vector data from the OpenStreeMap (OSM) Project and were downloaded for the whole state from the Geofabrik servers (https://download.geofabrik.de/) on the 25.05.2020.

Annual average surface temperatures (C°, mean of 2002-2012) with a spatial resolution of 250 x 250 m are based on MODIS data (Metz et al., 2014) and raster data is available processed and ready to use from the Hotmaps project (Fig. 2c, www.hotmaps.eu (accessed 28.05.2020)).

Terrestrial heat flow (W/m²) was interpolated from data available at the IHFC Global Heat Flow Database (https://ihfc-iugg.org/products/global-heat-flow-database) using the 2018 release, which is based on an earlier version (Global Heat Flow Compilation Group, 2013).

The maximum heat extraction rate (W/m borehole length) for different borehole lengths and usage times, as well as areas with restrictions for BHE installation (due to ground water protection areas or the presence of swellable rocks in the subsurface) were provided as raster data by the state office for geology, resources, and mining (Figs. 2a, b). This data is also accessible online in the information system for shallow geothermal energy (ISONG, https://isong.lgrb-bw.de/). ISONG data is based on a 3D geological model for the whole state of Baden-Württemberg, the maximum heat extraction data is calculated following VDI 4640. It is notable that for about 1/3 of the state's area BHE installations are restricted due to the geological setting or ground water protection areas.

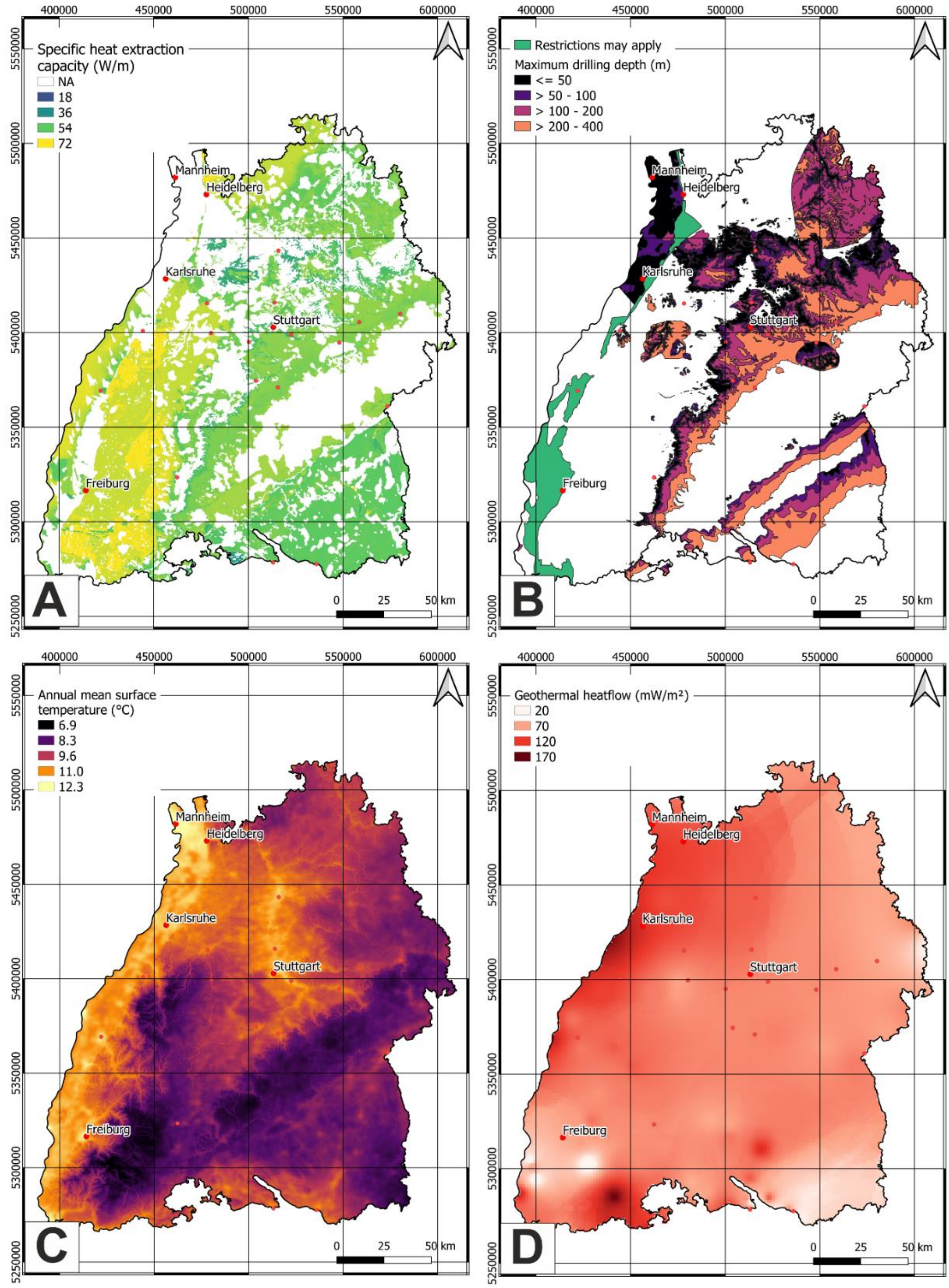

Figure 2: Maps illustrating input data. (A) Specific heat extraction capacity from ISONG. Note that white areas are groundwater protection areas where BHE installation is not allowed. These areas are not included in the study. (B) Maximum drilling depth and areas where the subsurface setting allows BHEs only after individual examination. (C) Annual mean surface temperature based on MODIS data. (D) Terrestrial geothermal heat flow from the global heat flow database.

2.3 Methods

2.3.1 Calculation of available space for BHEs

For the area of each building block (as defined in the Energieatlas) which does not fall into restricted regions (Fig. 2a), the area which could be used for BHE installation was determined by excluding buildings, roads and railways, footpaths and surface water (OSM data). A buffer of 3 m was placed around each building to ensure that BHEs could technically be placed, which is larger than the minimum distance of 2 m recommended by the German technical guideline VDI 4640 part 2 (VDI, 2019) and similar to other studies (Miglani et al., 2018; Zhang et al., 2014). As road and railway data is provided as vectors only, buffers were also placed around these, with the width of the buffer depending on the type of road as defined by OSM contributors. It is assumed that BHEs can be placed beneath pavements and parking areas (Zhang et al., 2014). In the resulting area per building block (Fig. 3) the maximum number of BHEs were distributed using a 10 m spacing, which is the minimum distance required by the regional law, and the QGIS “random points in polygons” algorithm. We use this approach instead of a grid-based approach often used in other studies (Schiel et al., 2016; Tissen et al., 2019b; Walch et al., 2021; Zhang et al., 2014) as this allowed for a better utilization of the available space. A total of 129.488 building blocks were analysed. The data used for BHE distribution and heat supply computations include raster, areal, and line data. Modification and computation of spatial data was done using QGIS (v. 3.14) and all input data was transformed into WGS 84 (EPSG:4326) prior to modification.

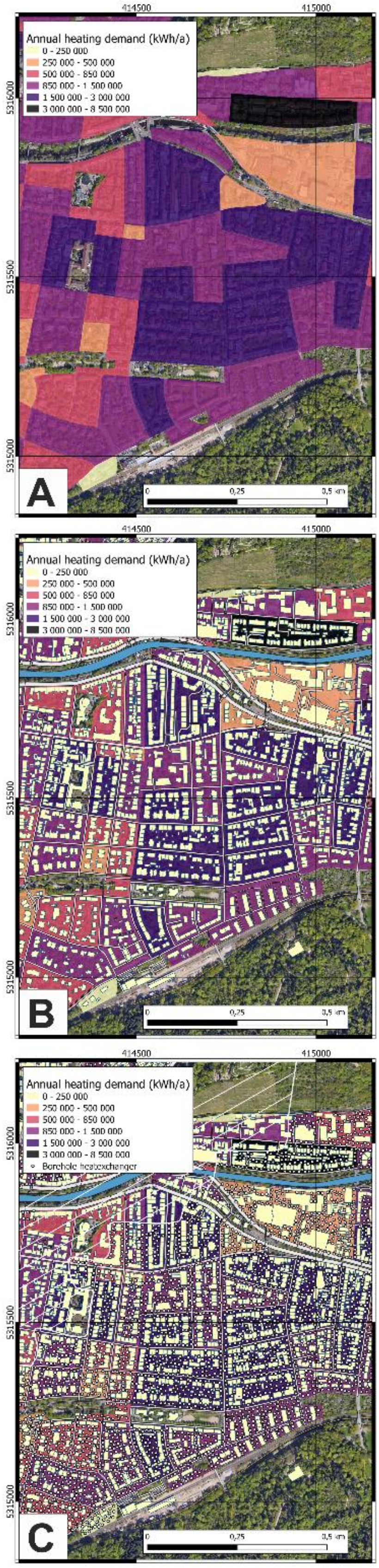

Figure 3: Maps illustrating the process of distributing BHEs: (A) shows the annual heating demand per building block. (B) For each building block unsuitable areas (buildings, roads, railways, waterways) are excluded. (C) BHEs are randomly distributed with a 10 m spacing to maximise the amount of BHEs available per building block. The striped area indicates a complex geological setting as defined by ISONG and thus this area is excluded from the study.

2.3.2 Calculation of the technical geothermal potential and heat supply rate

The geothermal potential of the BHEs fields and associated heat pumps are calculated for each field as follows (e.g. Tissen et al., 2019b):

$$E_{BHE} = \sum_{i}^{n} q_{BHE,i} \times l_{BHE,i} \times t_h / \left(1 - \frac{1}{COP}\right) \tag{1}$$

where q_{BHE} is the heat extraction rate of each BHE, l_{BHE} the length of each BHE, t_h is the operational time and COP the coefficient of performance of the heat pump. The heat extraction rate of each BHE in a steady state can be divided into three main components (Koenigsdorff, 2011):

$$q_{BHE}(t) = q_0 + q_p \times \sin\left(\frac{2\,\pi\,t}{t_p}\right) + q_{peak}(t) \tag{2}$$

Where q_0 is the stationary component, which includes the impact of the extraction rate on the subsurface over long periods of time as well as the interaction between multiple BHEs, q_p is the annual periodic component, which captures the fact that heating will mainly take place in the winter, and q_{peak} is the peak load over small periods of time. Each extraction component results in a change of the subsurface temperature at the borehole wall compared to the undisturbed subsurface temperature (T_0). The time-dependent change of the subsurface temperature (ΔT) depends on the dimensions of the BHE field and can be calculated using g-functions (Eskilson, 1987):

$$\Delta T = T_{BHE} - T_0 = \frac{q_{BHE}}{2\,\pi\,\lambda_e} \times g(Es, r_b/l, B/l) \tag{3}$$

with λ_e being the heat conductivity of the subsurface, g being the g-function which depends on the Eskilon number Es, which is the dimensionless ratio of real time to the physical time constant of the borehole, the ratio of BHE radius (r_b) to BHE length (l) and the ratio of BHE spacing (B) to BHE depth. In this study g-functions for each BHE field are estimated by using a range of stationary end values (ln(Es)=3) which depend on the number of BHEs in the field (Table 1). The undisturbed subsurface temperature T_0 can be estimated using mean annual surface temperature (T_s), the heat conductivity of the subsurface λ_e and the terrestrial heat flow density (q_{geo}):

$$T_0 \approx T_s + \frac{l}{2} \times \frac{q_{geo}}{\lambda_e} \tag{4}$$

While equation 3 calculates the temperature difference between borehole wall and the subsurface, the temperature difference between undisturbed soil and the borehole fluid (brine) is also of importance and can be calculated as follows:

$$\Delta T_{brine} = q_j \times (R_j + R_b) \tag{5}$$

Where q_j is one of the heat extraction components, R_j the correlating thermal resistivity, and R_b the borehole specific thermal resistivity which depends on the used cement and the borehole radius. The thermal resistivities R_0, R_p, and R_{peak} are functions of the borehole radius r_b and the heat conductivity of the subsurface λ_e and can be defined as follows (Eskilson, 1987; Koenigsdorff, 2011):

$$R_0 = \frac{1}{2\,\pi\,\lambda_e} \times \left[g(ln(Es) = 3, (r_b/l)) - \frac{r_b}{l \times 0.0005}\right] \tag{6}$$

Where the g function is taken from published tables (e.g. Eskilson, 1987).

$$R_p = \frac{1}{2\,\pi\,\lambda_e} \times \sqrt{(ln\left(\frac{2}{r_{pb}}\right) - \gamma)^2 + \frac{\pi}{16}} \; with \;\; r_{pb} = r_b \times \sqrt{2}/d_p \; and \;\; d_p = \sqrt{a \times t_p/\pi} \tag{7}$$

$$R_{peak} = \frac{1}{2\,\pi\,\lambda_e} \times \left[ln\left(\frac{\sqrt{4\ \times a \times t_{peak}}}{r_b} \right) - \gamma/2 \right] \quad (8)$$

With a being the thermal conductivity of the subsurface:

$$a = \frac{\lambda_e}{\rho_e\ \times c_p} \quad (9)$$

For this study the volumetric heat capacity (ρ_e x c_p) is assumed to be 2.18 MJ/(m³/K) (Koenigsdorff et al., 2006). Based on equations 1-9 an R code, similar to the GEO-HAND^{light} tool (https://innosued.de/energie/geothermie-software-2/), was developed. It optimizes heat extraction rates from a given borehole field while taking the guideline VDI 4640 (VDI, 2019) as well as state specific guidelines on BHEs (Baden-Württemberg, 2018) into account. These include that the maximum temperature difference between brine when it enters the borehole and the undisturbed subsurface temperature cannot exceed 17 °K and that the same temperature difference during continuous operation may not exceed 11 °K. Additionally, the temperature of brine entering the borehole may not be below -3°C to prevent freezing of the subsurface. For simplicity, the conservative model assumes no groundwater flow, and within each building block the geological data is assumed to be constant, which is true for >95% of cases.

Besides the maximum geothermal potential (E_{max}), which utilizes all placeable BHEs of a building block, the number of BHEs needed to supply heat for the three different heating demand scenarios (see section 2.2.) as well as the number of BHEs needed per building for each of these scenarios were calculated.

Table 1: Parameters used to determine heat extraction rates.

Parameter	**Value**		**Source**
COP	4.3		State guidelines
BHE length (l)	max = 100 m		ISONG
BHE spacing (B)	10 m		State guidelines
BHE radius (r_b)	0.065 m		DN40 U pipe
Heat extraction rate (q)	23-72 W/m		Target variable
Operation (t)	1800 h/year		Heating only
Volumetric heat capacity (ρ_e c_p)	2.18 MJ/(m³/K)		Koenigsdorff et al., 2006
Heat conductivity (λ)	2.25 W/mK		Simplified after ISONG
Thermal resistivity borehole	0.1 mK/W		
t_p	8760 h		One year
t_{peak}	24 h		One day
g-functions (ln(Es)=3, rb/H = 0.0005, B/H)	No. BHEs	Value	
	1	6.6	
	2	7.2	
	2-5	9	
	5-16	12.2	
	16-18	13.7	
	18-50	17.8	

	50-100	21	
	100-150	30	
	>150	50	

3 Results and discussion

3.1 BHE placement

In the 129.488 building blocks a total of around 6.426.000 BHEs could be placed, with an average of 49.6 BHEs per building block and a median of 39 BHEs per building block (Fig. 4a). Considering that the area of building blocks varies from less than 500 m² to close to 1 million m², analysing the number of BHEs per hectar gives a better understanding of the BHE density, which averages at 43.6 BHEs per hectare and has a median of 46.5 BHEs per hectare (Fig. 4b). The vast majority of BHEs has a depth of 100 m with only around 40.000 BHEs being in areas where the drilling depth is limited to 50 m.

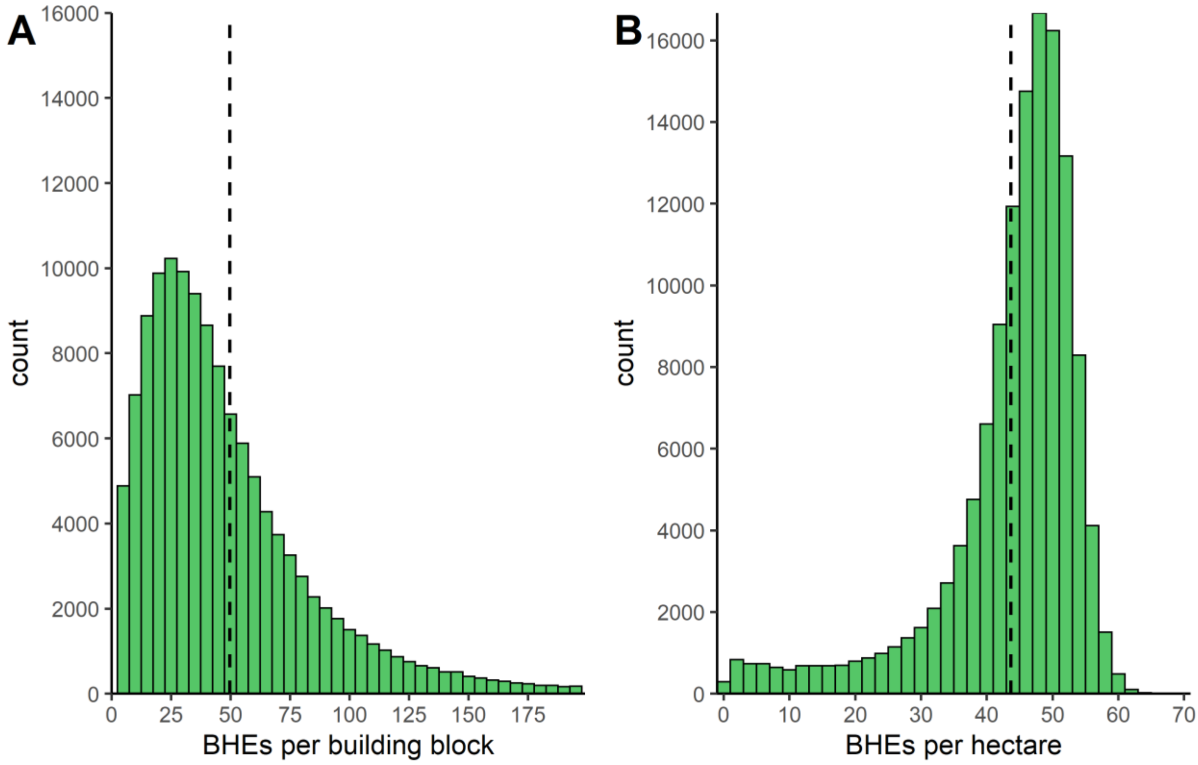

Figure 4: Histograms illustrating (A) the number of BHEs per building block and (B) the number of BHEs per building block normalized to area. Dashed lines indicate the mean number of BHEs.

Utilizing OSM data for renewable energy planning is widely used when more detailed official standardized data is not available (Alhamwi et al., 2017; Chu and Hawkes, 2020), however it comes with limitations. In our study a buffer of the same width was placed around all roads of the same OSM class and thus it is assumed that all roads of the same type have the same width in the whole study area. While cross-checks with satellite imagery show that in most cases the used width is acceptable, there are instances where roads are much wider or smaller than assumed in the model. This subsequently impacts the number of BHEs which are placeable within the building blocks affected. It should also be noted that the building block area defined by the Energieatlas, which is the area used to distribute BHEs, generally does not extend more than a few meters from the buildings within the building block. However, for building blocks located at the edge of villages or cities, adjacent undeveloped space could be used for BHE placement. This would significantly increase the number of potentially placable BHEs.

3.2 Technical geothermal potential

The technical geothermal potential of building blocks ranges from 0 to more than 600.000 kWh per year, and averages at 257.000 kWh per year and hectare when the building block areas are normalised (Fig. 5). Overall, the technical geothermal potential of the whole state yields an annual total of 33.5 TWh. There are no regional trends visible within the geothermal potential and the geothermal potential of a building block is largely controlled by the building density of the building block, with building blocks with a high number of buildings per hectare having a low geothermal potential and building blocks with a low building density exhibiting high geothermal potentials (Fig. 6). City centres with a high building density thus have a low geothermal potential while residential areas at the fringes of a city or in rural areas generally have higher geothermal potentials (Fig. 7).

The technical geothermal potential with a mean of 25.7 kWh/m²/a (Fig. 5b) is in the same order of magnitude as the technical geothermal potential of a regional study in Northern Switzerland where Walch et al. (2021) estimate it to be 16.4 kWh/m²/a. The difference is likely due to a range of factors, including differences in the geological settings, the BHE distribution algorithm, as well as the correction for thermal interference between neighbouring BHEs and BHE fields. The fact that the technical geothermal potential correlates with the building density of the building blocks is not surprising, as building blocks with few buildings generally have more space available for BHEs. To identify areas which are well suited for GSHPs to supply heat using building density may thus be a good approach.

Identified technical geothermal potentials are likely to be underestimated for the rural areas and slightly overestimated in urban areas due to the BHE placing method and its shortcomings. It should be noted that groundwater flow has been excluded from this study, as this is quite complex on a regional scale. Consideration of groundwater flow would increase the technical geothermal potential for most building blocks which would similarly increase (up to 40 %) for urban areas if the urban heat island effect would be included (Menberg et al., 2013; Rivera et al., 2017). While our modelling approach takes the thermal interference of neighbouring BHEs into account, which is often not considered even on a district (Tissen et al., 2019b; Zhang et al., 2014) or city scale (Schiel et al., 2016), it does so by using an estimated g-function based on the number of BHEs per building block. It thus does not consider the effect of BHEs on neighbouring building blocks which will also interfere. Future work should thus include this effect and may also calculate the true interference per building block by calculating the g-function for each BHE field, e.g. using available Python libraries (Cimmino, 2018). Overall, the technical geothermal potentials provided in this study are conservative estimates which can be used for regional and local planning of using renewable heating energy but are no replacement for a detailed study prior to constructing individual BHE fields.

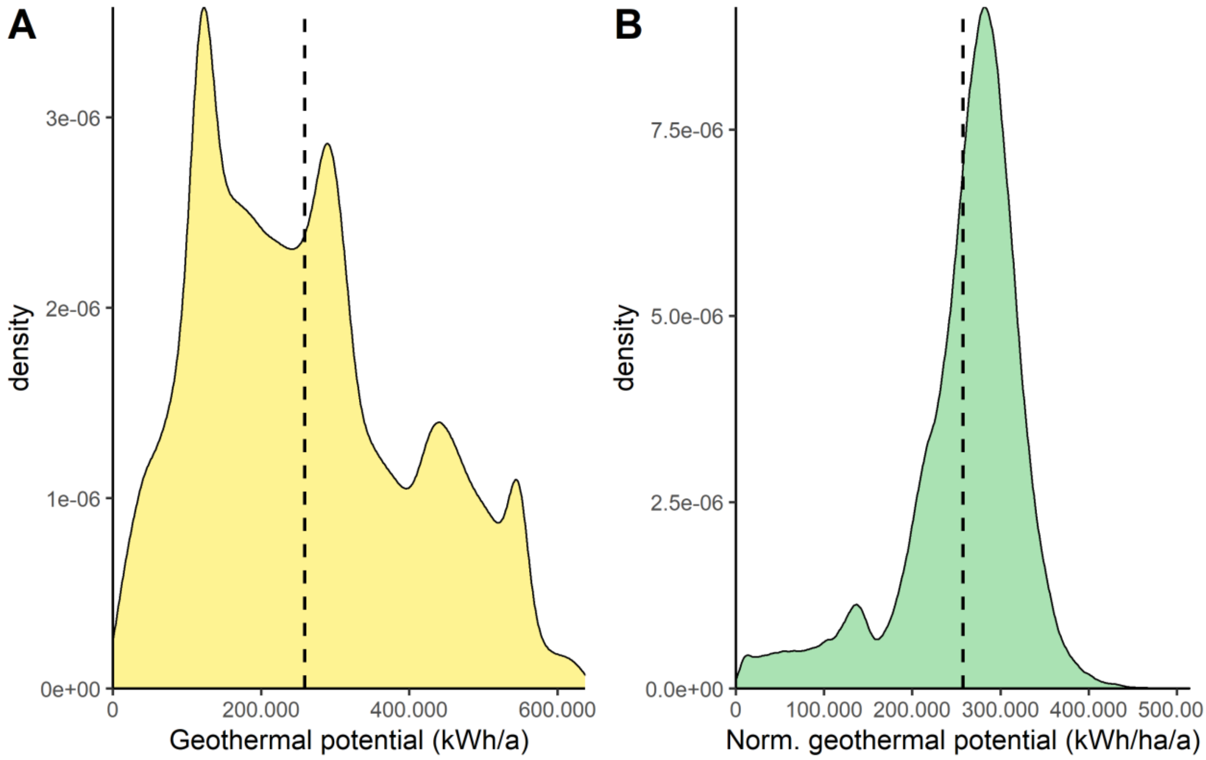

Figure 5: Density plots showing (A) the geothermal potential per building block and (B) the geothermal potential normalised to area (hectars). Dashed lines indicate the mean geothermal potential.

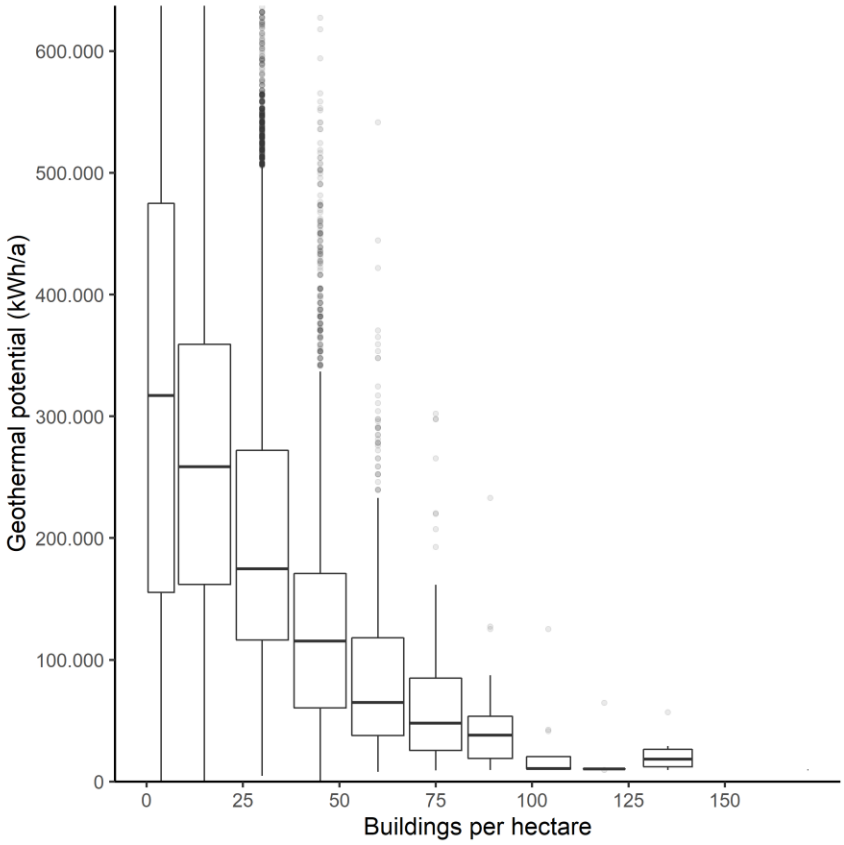

Figure 6: Boxplot illustrating that the geothermal potential per building block is largely dependent on the building density, with building blocks with a low building density generally exhibiting higher geothermal potentials than building blocks with a high building density.

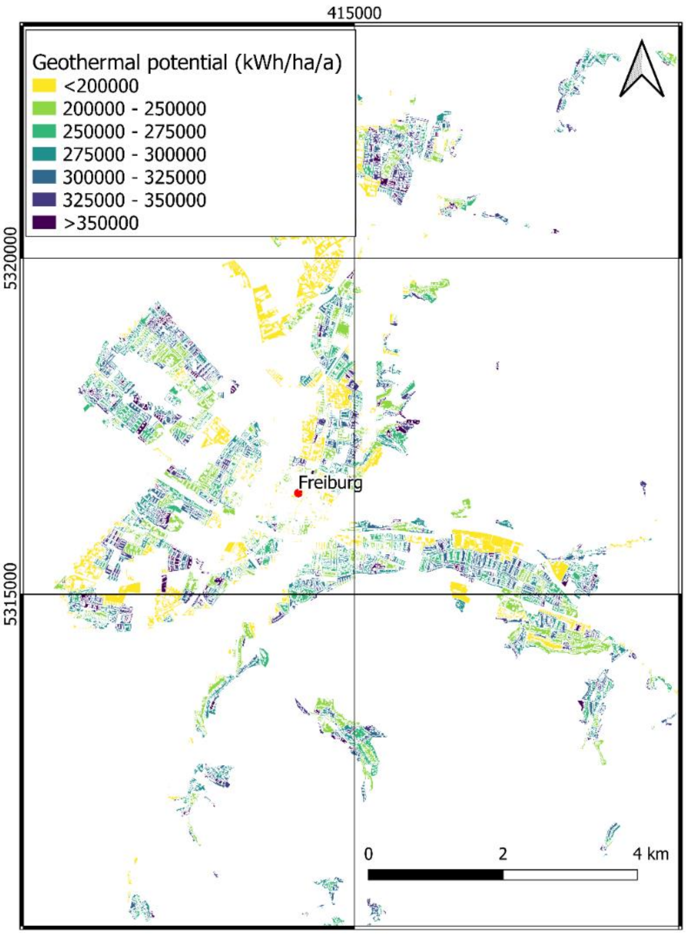

Figure 7: Map illustrating the geothermal potential for parts of the city of Freiburg. Note how the centre of town (around the town name) has a low potential while residential areas at the edge of town have higher potentials.

3.3 Heating supply rates

The geothermal potential per building block calculated above can be contrasted with the heating demand of the different building status scenarios included in the Energieatlas data (Fig. 8). For the heating demand scenario “as is” the heating demand of about 44 % of all building blocks can be covered by GSHPs alone. This number increases to 65 % in the “conventional renovation” scenario and to 93 % of all building blocks in the “forward-looking renovation” scenario. While in the “as is” scenario mainly building blocks with a low heating demand can be supplied exclusively by GSHPs, in the “forward-looking renovation” scenarios even building blocks with a heating demand of 1000 MWh/a can be heated solely by GSHPs (Fig. 9). The number of BHEs needed to successfully heat a building exclusively by shallow geothermal energy also drastically decreases from the “as is” with a mean of 6.2 BHEs to the “forward-looking renovation” scenario where on average only 1.3 BHEs per building are needed (Fig. 10).

On a regional scale it becomes clear that the minimum drilling depth exerts a strong control whether the heat demand of a building block can be covered by GSHPs or not: for the “as is” and “conventional renovation” scenarios many of the building blocks for which heat demand cannot be covered by GSHPs are located in the South German Scarpland around Stuttgart where maximum drilling depth is often restricted to 50 m (Fig. 11, Fig. 2b). Additionally, building blocks for which heat cannot be supplied only by GSHPs in all scenarios are located in densely populated areas.

The heating supply rates of 44 % for the "as is" building renovation scenario is similar to what has been observed in other studies for urban areas: Schiel et al. (2016) estimate 40 % of parcels in a German urban area could be supplied with GSHPs while Zhang et al. (2014) report that 69 % of the heating demand of the district of Westminster, UK, could be supplied by GSHPs. For another urban quarter in Germany Tissen et al. (2019b) estimate 22-34 % of the heating demand could be supplied by BHEs before and 47-71 % after building renovation. It is noteworthy that in our study not only urban quarters but also rural areas are included and the heating supply rate still does not increase. This is likely due to the fact that the heating supply for the "as is" scenario in urban areas comes closer to the study of Tissen et al (2019) and is significantly higher in rural areas. The higher heating supply rates of 65 % and 93 % for the renovated building scenarios are in line with the results of Tissen et al. (2019). The significant decrease in needed BHEs per building to cover the heating demand in the "forward-looking renovation" scenario as compared to the "as is" scenario is also interesting from a cost perspective: the on average five saved BHEs per building would, when construction costs of 60 €/m are assumed, save 30.000 € of BHE installation cost per building which could be invested into the building renovation.

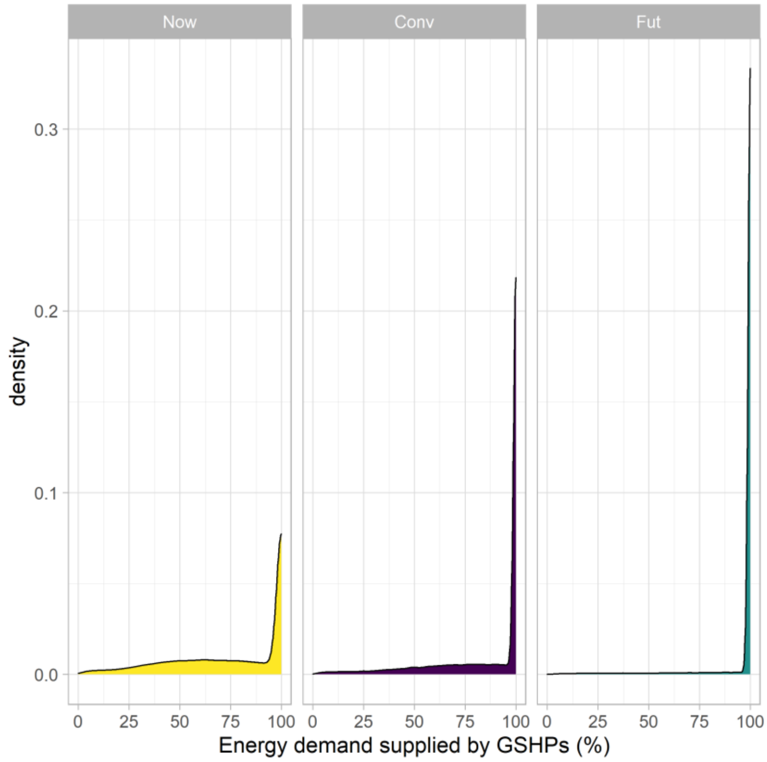

Figure 8: Density plots of the annual heating demand of all building blocks covered by GSHPs for the three demand scenarios (Now= "As-is", Conv ="Conventional renovation", Fut ="forward-looking renovation").

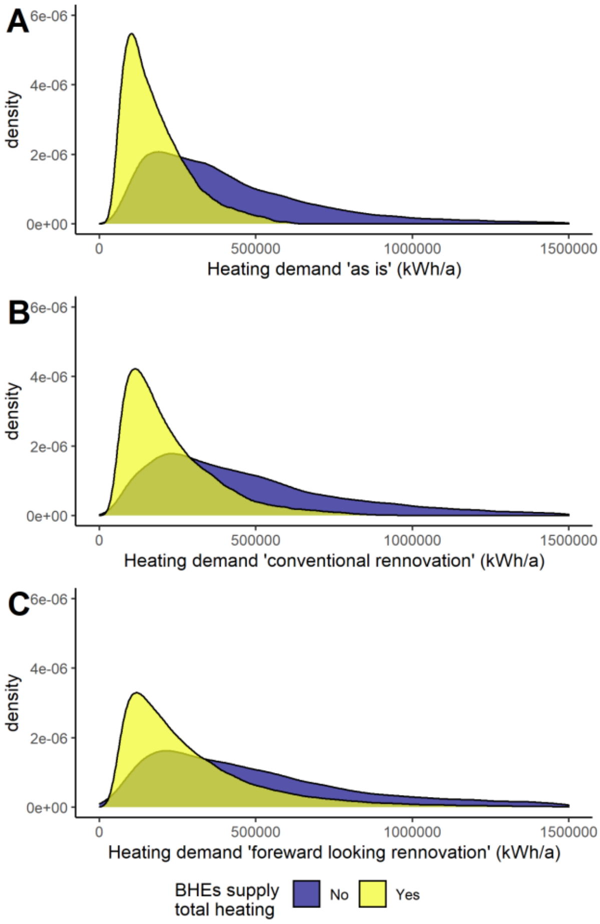

Figure 9: Density plots illustrating the heating demand of building blocks where BHEs can supply to total heating demand for the three different energy demand scenarios.

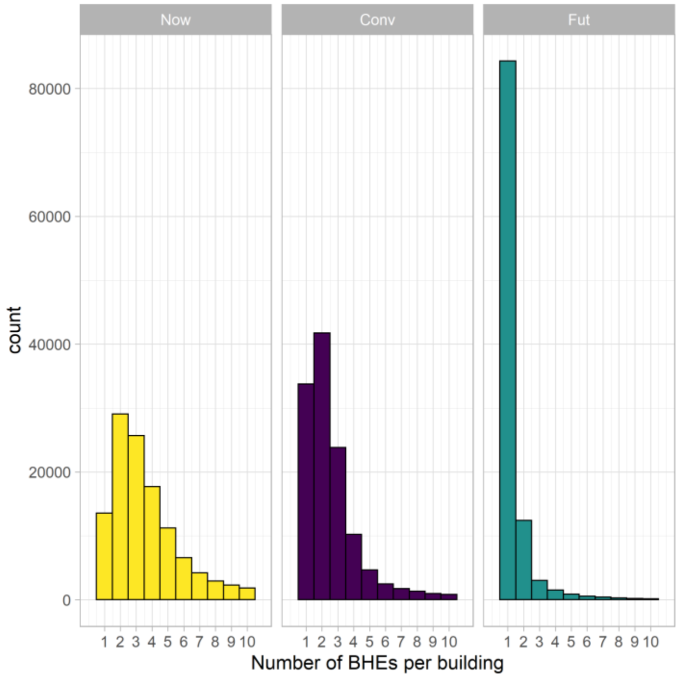

Figure 10: Barplots illustrating the number of BHEs needed per building to cover the heat demand for the three different renovation scenarios. Note how forward-looking renovations (Fut) decrease the amount of BHEs needed drastically (Now= “As-is”, Conv =”Conventional renovation”, Fut =”forward-looking renovation”).

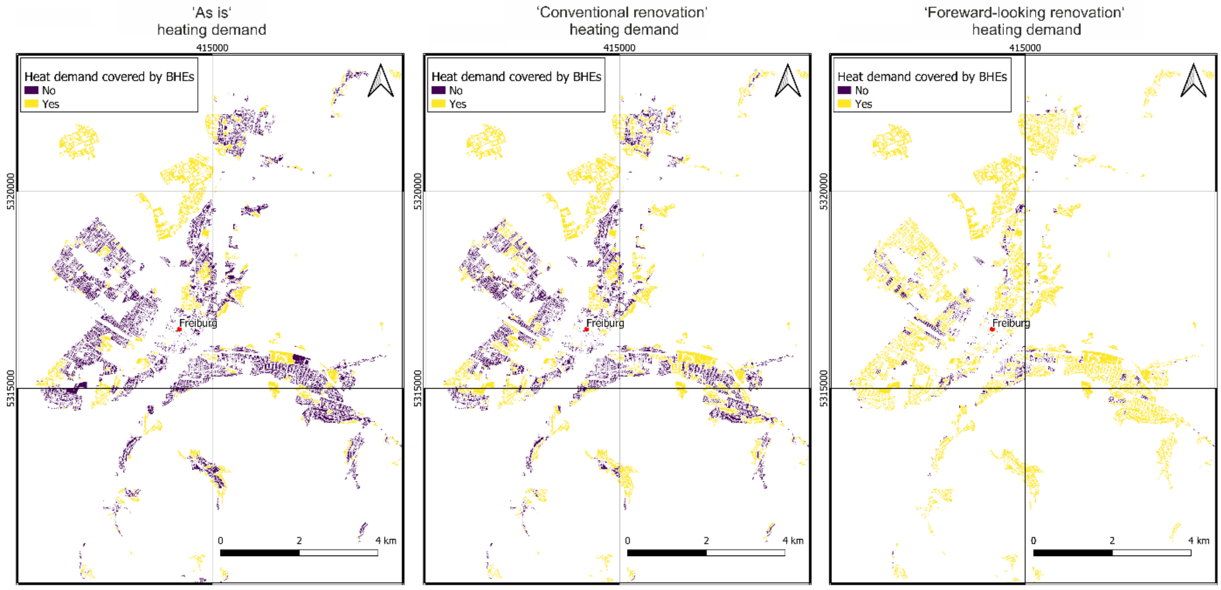

Figure 11: Maps illustrating for which building blocks of the city of Freiburg heat demand can be covered by GSHPs for the three different heat demand scenarios.

4 Practical implications and future work

Regional scale estimations of the technical geothermal potential are required for urban and rural planning, policy making, and the development of regulations (Walch et al., 2021). For the state of Baden-Württemberg large municipalities with more than 20.000 inhabitants must develop a heating plan which will form the base for climate-neutral heating supply in 2050. The geothermal potential and heating supply rates provided in this study will assist the urban planners and policy makers involved in the heating plan development to estimate the potential of GSHPs in any neighbourhood in the state. Additionally, it can be used to identify (urban) areas in which GSHPs are no option even for renovated buildings due to the building density and geological setting and where other means of heat supply will be needed. To ensure access to the data from this study it will be stored with the state energy bureau which will provide it to the municipalities.

Future work will aim to improve the estimation of a technical geothermal potential on a large scale (state, country) by addressing several of the limitations highlighted in this study, including using official land register data for BHE distribution, implementing heat transfer from groundwater flow in the model as well as including the urban heat island effect. For areas in which BHE are not an option due to groundwater protection areas or due to the geological setting the use of horizontal shallow geothermal systems should be analysed. Other practical factors such as additional costs arising from using drilling equipment on steep slopes and the suitability of the building ground should also be considered. Understanding and quantifying the uncertainties of all included data and the modelling approach will also significantly improve the reliability of the technical geothermal potential on a regional scale. By using machine learning approaches the (geological) input data needed for the model may be estimated on a regional (Bourhis et al., 2021) or country (Assouline et al., 2019) scale, which indicates that continental scale technical geothermal potential studies are possible in the near future.

Heating demand data, which is necessary for heating plan development and the utilization of renewable technologies, also must be improved. The heating demand scenarios used in this study can only be the first step towards more detailed models in which the true demand of each residential building is included. Energy efficiency renovations to the “forward-looking renovation” standard used in this study may not be realizable for reasonable costs for many buildings, particularly of half-timbered buildings which are common in Central Europe.

5 Conclusions

In this study the technical geothermal potential from ground-source heat pumps for individual building-blocks on a regional scale is estimated and the thermal energy that these vertical borehole heat exchangers is linked to the heat demand of the individual building blocks for different demand scenarios. The proposed method to estimate the geothermal potential takes the available area for borehole installation, the technical and geological parameters of the boreholes, and the thermal interference between boreholes into account as well as restrictions on borehole and heat extraction parameters governed by state and federal law.

Our results provide a first estimate of the technical potential of shallow geothermal energy in the state of Baden-Württemberg. Depending on the demand scenario between 44 % and 97 % of all building blocks can be supplied with sufficient energy from ground-source heat pumps. Particularly rural and suburban areas have high heating supply rates even in high demand scenarios. This work can be used to assess the techno-economic aspects of a wide-spread rollout of borehole heat exchangers and will be used for the required heating plans each municipality in the state has to develop. As such is contributes to the development of low-carbon heating sectors in Baden-Württemberg by highlighting where shallow geothermal energy can play a larger role and by highlighting (urban) areas where other heat sources, such as district heating networks, are needed.

Acknowledgments

JMM was partly funded by the RES_TMO project, which is co-funded by the EU programme Interreg V Upper Rhine through the European Regional Development Fund (EFRE/FEDER) for the period 1.02.2019 – 31.01.2022 under the grant reference (Ref: 4726/6.3.).

References

Alhamwi, A., Medjroubi, W., Vogt, T., Agert, C., 2017. GIS-based urban energy systems models and tools: Introducing a model for the optimisation of flexibilisation technologies in urban areas. Applied Energy 191, 1–9. https://doi.org/10.1016/j.apenergy.2017.01.048

Assouline, D., Mohajeri, N., Gudmundsson, A., Scartezzini, J.-L., 2019. A machine learning approach for mapping the very shallow theoretical geothermal potential. Geothermal Energy 7, 19. https://doi.org/10.1186/s40517-019-0135-6

Baden-Württemberg, 2018. Leitlinien Qualitätssicherung Erdwärmesonden (LQS EWS).

Bayer, P., Attard, G., Blum, P., Menberg, K., 2019. The geothermal potential of cities. Renewable and Sustainable Energy Reviews 106, 17–30. https://doi.org/10.1016/j.rser.2019.02.019

Bertermann, D., Klug, H., Morper-Busch, L., 2015. A pan-European planning basis for estimating the very shallow geothermal energy potentials. Renewable Energy 75, 335–347. https://doi.org/10.1016/j.renene.2014.09.033

Bourhis, P., Cousin, B., Rotta Loria, A.F., Laloui, L., 2021. Machine learning enhancement of thermal response tests for geothermal potential evaluations at site and regional scales. Geothermics 95, 102132. https://doi.org/10.1016/j.geothermics.2021.102132

Casasso, A., Sethi, R., 2016. G.POT: A quantitative method for the assessment and mapping of the shallow geothermal potential. Energy 106, 765–773. https://doi.org/10.1016/j.energy.2016.03.091

Chu, C.-T., Hawkes, A.D., 2020. A geographic information system-based global variable renewable potential assessment using spatially resolved simulation. Energy 193, 116630. https://doi.org/10.1016/j.energy.2019.116630

Cimmino, M., 2018. Fast calculation of the g-functions of geothermal borehole fields using similarities in the evaluation of the finite line source solution. Journal of Building Performance Simulation 11, 655–668. https://doi.org/10.1080/19401493.2017.1423390

Eskilson, P., 1987. Thermal analysis of heat extraction boreholes (PhD). University of Lund, Lund.

European Parliament, 2020. The European Green Deal European Parliament resolution of 15 January 2020 on the European Green Deal (2019/2956(RSP)).

Fleiter, T., Elsland, R., Rehfeldt, M., al, et, 2017. Profile of heating and cooling demand in 2015. Karlsruhe.

Galgaro, A., Di Sipio, E., Teza, G., Destro, E., De Carli, M., Chiesa, S., Zarrella, A., Emmi, G., Manzella, A., 2015. Empirical modeling of maps of geo-exchange potential for shallow geothermal energy at regional scale. Geothermics 57, 173–184. https://doi.org/10.1016/j.geothermics.2015.06.017

Geyer, M., Nitsch, E., Simon, T., Geyer, O.F., Gwinner, M.P., 2011. Geologie von Baden-Württemberg, 5th ed. Schweizerbart'sche, E., Stuttgart.

Global Heat Flow Compilation Group, 2013. Component parts of the World Heat Flow Data Collection. https://doi.org/10.1594/PANGAEA.810104

Koenigsdorff, R., 2011. Oberflächennahe Geothermie für Gebäude. Frauenhofer IRB.

Koenigsdorff, R., Heinrich, S., Sedlak, M., 2006. Test und Weiterentwicklung des Progamms GEOSYST und Bemessung von Erdwärmesondenfeldern mit einem daraus abgeleiteten Handrechenverfahren. Presented at the Otti-Profiforum Oberflächennahe Geothermie, Freising.

Krecher, M., Vorstellung eines „Erdwärmescreenings" als ganzheitliche Planungsgrundlage für den Ausbau der Geothermie (Beispiel: Südlicher Oberrhein). M.Sc. Thesis, University of Koblenz-Landau, pp. 146.

KSG BW, 2013. Landesrecht BW KSG BW | Landesnorm Baden-Württemberg | Gesamtausgabe | Klimaschutzgesetz Baden-Württemberg (KSG BW) vom 23. Juli 2013 | gültig ab: 31.07.2013.

Li, M., Li, P., Chan, V., Lai, A.C.K., 2014. Full-scale temperature response function (G-function) for heat transfer by borehole ground heat exchangers (GHEs) from sub-hour to decades. Applied Energy 136, 197–205. https://doi.org/10.1016/j.apenergy.2014.09.013

Lund, H., 2007. Renewable energy strategies for sustainable development. Energy, Third Dubrovnik Conference on Sustainable Development of Energy, Water and Environment Systems 32, 912–919. https://doi.org/10.1016/j.energy.2006.10.017

Lund, H., Möller, B., Mathiesen, B.V., Dyrelund, A., 2010. The role of district heating in future renewable energy systems. Energy 35, 1381–1390. https://doi.org/10.1016/j.energy.2009.11.023

Lund, J.W., Boyd, T.L., 2016. Direct utilization of geothermal energy 2015 worldwide review. Geothermics 60, 66–93. https://doi.org/10.1016/j.geothermics.2015.11.004

Luo, J., Luo, Z., Xie, J., Xia, D., Huang, W., Shao, H., Xiang, W., Rohn, J., 2018. Investigation of shallow geothermal potentials for different types of ground source heat pump systems (GSHP) of Wuhan city in China. Renewable Energy 118, 230–244. https://doi.org/10.1016/j.renene.2017.11.017

Majorowicz, J., Grasby, S.E., Skinner, W.R., 2009. Estimation of Shallow Geothermal Energy Resource in Canada: Heat Gain and Heat Sink. Nat Resour Res 18, 95–108. https://doi.org/10.1007/s11053-009-9090-4

Menberg, K., Bayer, P., Zosseder, K., Rumohr, S., Blum, P., 2013. Subsurface urban heat islands in German cities. Science of The Total Environment 442, 123–133. https://doi.org/10.1016/j.scitotenv.2012.10.043

Meng, B., Vienken, T., Kolditz, O., Shao, H., 2019. Evaluating the thermal impacts and sustainability of intensive shallow geothermal utilization on a neighborhood scale: Lessons learned from a case study. Energy Conversion and Management 199, 111913. https://doi.org/10.1016/j.enconman.2019.111913

Metz, M., Rocchini, D., Neteler, M., 2014. Surface Temperatures at the Continental Scale: Tracking Changes with Remote Sensing at Unprecedented Detail. Remote Sensing 6, 3822–3840. https://doi.org/10.3390/rs6053822

Miglani, S., Orehounig, K., Carmeliet, J., 2018. A methodology to calculate long-term shallow geothermal energy potential for an urban neighbourhood. Energy and Buildings 159, 462–473. https://doi.org/10.1016/j.enbuild.2017.10.100

Noorollahi, Y., Gholami Arjenaki, H., Ghasempour, R., 2017. Thermo-economic modeling and GIS-based spatial data analysis of ground source heat pump systems for regional shallow geothermal mapping. Renewable and Sustainable Energy Reviews 72, 648–660. https://doi.org/10.1016/j.rser.2017.01.099

Orehounig, K., Evins, R., Dorer, V., 2015. Integration of decentralized energy systems in neighbourhoods using the energy hub approach. Applied Energy 154, 277–289. https://doi.org/10.1016/j.apenergy.2015.04.114

Patton, A.M., Farr, G., Boon, D.P., James, D.R., Williams, B., James, L., Kendall, R., Thorpe, S., Harcombe, G., Schofield, D.I., Holden, A., White, D., 2020. Establishing an urban geo-observatory to support sustainable development of shallow subsurface heat recovery and storage. Quarterly Journal of Engineering Geology and Hydrogeology 53, 49–61. https://doi.org/10.1144/qjegh2019-020

Rivera, J.A., Blum, P., Bayer, P., 2017. Increased ground temperatures in urban areas: Estimation of the technical geothermal potential. Renewable Energy 103, 388–400. https://doi.org/10.1016/j.renene.2016.11.005

Schiel, K., Baume, O., Caruso, G., Leopold, U., 2016. GIS-based modelling of shallow geothermal energy potential for CO2 emission mitigation in urban areas. Renewable Energy 86, 1023–1036. https://doi.org/10.1016/j.renene.2015.09.017

Schweizer, I., 2019. Entwicklung des Energieverbrauchs in Baden-Württemberg Ergebnisse der Energiebilanzen. Statistisches Monatsheft Baden-Württemberg 51–59.

Tissen, C., Benz, S.A., Menberg, K., Bayer, P., Blum, P., 2019a. Groundwater temperature anomalies in central Europe. Environ. Res. Lett. 14, 104012. https://doi.org/10.1088/1748-9326/ab4240

Tissen, C., Menberg, K., Bayer, P., Blum, P., 2019b. Meeting the demand: geothermal heat supply rates for an urban quarter in Germany. Geothermal Energy 7, 9. https://doi.org/10.1186/s40517-019-0125-8

Tissen, C., Menberg, K., Benz, S.A., Bayer, P., Steiner, C., Götzl, G., Blum, P., 2021. Identifying key locations for shallow geothermal use in Vienna. Renewable Energy 167, 1–19. https://doi.org/10.1016/j.renene.2020.11.024

UNFCCC, 2015. Adoption of the Paris Agreement.

VDI (Ed.), 2019. VDI 4640 Blatt 2 - Thermische Nutzung des Untergrunds - Erdgekoppelte Wärmepumpenanlagen. VDI-Gesellschaft Energie und Umwelt.

Vienken, T., Schelenz, S., Rink, K., Dietrich, P., 2015. Sustainable Intensive Thermal Use of the Shallow Subsurface—A Critical View on the Status Quo. Groundwater 53, 356–361. https://doi.org/10.1111/gwat.12206

Walch, A., Mohajeri, N., Gudmundsson, A., Scartezzini, J.-L., 2021. Quantifying the technical geothermal potential from shallow borehole heat exchangers at regional scale. Renewable Energy 165, 369–380. https://doi.org/10.1016/j.renene.2020.11.019

Zhang, C., Wang, Y., Liu, Y., Kong, X., Wang, Q., 2018. Computational methods for ground thermal response of multiple borehole heat exchangers: A review. Renewable Energy 127, 461–473. https://doi.org/10.1016/j.renene.2018.04.083

Zhang, Y., Soga, K., Choudhary, R., 2014. Shallow geothermal energy application with GSHPs at city scale: study on the City of Westminster. Géotechnique Letters 4, 125–131. https://doi.org/10.1680/geolett.13.00061